Brabender®

Polymer Processing Solutions

Twin Screw and Single Screw Applications

MetaStation 4E

Tabletop Drive Unit

TwinLab C

Standalone Twin Screw

Advantages:

- **Small sample sizes for multiple tests per day**
- **Clamshell barrel and segmented screw designs**
- **Small laboratory footprint**

follow us

Brabender® 5-Star Service

Received: 25 April 2020 | Revised: 13 June 2020 | Accepted: 16 June 2020

DOI: 10.1002/pc.25716

RESEARCH ARTICLE

Polymer COMPOSITES WILEY

Investigation of surface-pegylated nanocellulose as reinforcing agent on PBAT biodegradable nanocomposites

Alana Gabrieli de Souza[1] | **Giovanni Floriano de Lima**[1] | **Vijaya Kumar Rangari**[2] | **Derval dos Santos Rosa**[1]

[1]Centro de Engenharia, Modelagem e Ciências Sociais Aplicadas—CECS, Universidade Federal do ABC (UFABC), Santo André, Sao Paulo, Brazil

[2]Department of Materials Science and Engineering, Tuskegee University, Tuskegee, Alabama

Correspondence
Derval dos Santos Rosa, Centro de Engenharia, Modelagem e Ciências Sociais Aplicadas—CECS, Universidade Federal do ABC (UFABC), Avenida dos Estados, 5001, CEP: 09210-580, Santo André, Sao Paulo, Brazil.
Email: dervalrosa@yahoo.com.br; derval.rosa@ufabc.edu.br

Funding information
Fundação de Amparo à Pesquisa do Estado de São Paulo, Grant/Award Numbers: 2018/11277-7, 2018/25239-0, 22035-4; NSF-CREST, Grant/Award Number: 1735971

Abstract

In the present work, nanocellulose (NC) has been surface-pegylated and further employed as reinforcement in poly(butylene adipate-co-terephthalate) (PBAT) through the melting process. The nanocomposites showed a significant stiffness increase, especially the 2% pegylated-NC, due to the good interaction between the modified NC and the matrix. Also the pegylation improved the filler-PBAT adhesion, which resulted in higher thermal stability and low crystallinity. Raman spectroscopy confirmed the strong interaction between the 2% pegylated-NC, morphological analysis confirmed the filler adhesion. The water absorption indicated that the pegylated-NC has a low tendency to absorb water, which improves its applicability, for example, as a packaging material. This unique study is of great value for the future design of pegylated-NC biodegradable nanocomposites with tailored properties.

KEYWORDS

biodegradable, composites, modification, nanotechnology

1 | INTRODUCTION

Biodegradable nanocomposites are a new class of biopolymers that has attracted attention in the last decade. [1] These materials highlighted due to their nontoxicity and the wide range of applications. They are usually composed of fillers, additives, nanoparticles (especially the nanocelluloses [NCs]), and a biodegradable polymer.[2] Among the biodegradable polymers, poly(butylene adipate-co-terephthalate) (PBAT) highlights because of its easy processing and adequate thermal properties. [3] However, due to their poor mechanical and thermomechanical properties, reinforcing agents could improve the polymer properties to meet desired applications. [4–7]

NCs are rigid particles, and among their attractive features are renewability, biocompatibility, sustainability, low density, high crystallinity, and high specific strength and modulus. [1,8] Several studies report the use of NC as reinforcement in different polymer matrices, since its unique properties make these materials more efficient.[9–11] NCs show the opportunity to obtain high mechanical performance from renewable and high available material.[10] Also, authors demonstrate that NCs are potential reinforcing agents in biodegradable polymer matrices because they improve their performance during the use of the material, and after disposal, they are completely biodegradable, even being able to accelerate the biodegradation process.[12–14] However, the reinforcing effect often depends on the dispersion and interaction between the filler and the polymer matrix. [6,15,16]

Although NCs have active groups on their surface, their hydrophilic character results in high agglomeration tendency and limits its dispersion on polymeric matrices. Besides, the most used biodegradable polymers are

hydrophobic and nonpolar, such as PBAT and PBS, limiting their performance as nanofillers. [17,18] Literature reports the NC chemical or physical surface modification to achieve good dispersion and adhesion in the nonpolar matrices. [4,6,19–22] It is well known that the good reinforcement effect is attributed to the formation of a rigid NC percolating network within the polymer matrix through strong interaction between the materials. The NC-polymer matrix interaction is also important for mechanical improvements because such interaction facilitates load transfer between the filler and the matrix. [23,24]

Different approaches can achieve the NC dispersion, such as homo- or block-copolymers to improve the steric stabilization; [25,26] surfactant-assisted dispersion; [27–29] acetylation; [30] solvent-assisted dispersion (the NCs are solvent exchanged from water to DMSO or DMF, for example, it is a high-cost and lead to environmental emission and human exposure of volatile organic compounds); [22] freeze-dry of the NCs; grafting with low average molecular weight polymers. [24,31,32] However, most approaches have high economic and environmental impacts, generating toxic by-products, and limiting the application in biomaterials, for example.

There have been several previously reported NC/PBAT nanocomposite studied utilizing some of the strategies stated above. [33–38] Besides, some authors investigated the use of polyethylene glycol (PEG) as a compatibilizer for cellulose microfibers. Moustafa et al prepared torrefied coffee grounds PBAT composites and observed that the torrefaction improved the available hydroxyl groups of cellulose, resulting in composites with superior mechanical, thermal, and crystalline properties. [39] Moustafa, Guizani, and Dufresne prepared composites using coffee grounds in the microscale, and extruded composites of cellulose/PBAT/PEG.[40] The authors observed that the coffee grounds showed good interaction with the PEG matrix, which acted as a plasticizer phase, and investigated the thermal degradation kinect. Despite the indications that PEG may be a good compatibilizer between the PBAT and cellulose matrix, no records report the use of PEG in PBAT/NC nanocomposites.

The literature reports the development of PBAT/PEG blends reinforced with cellulose particles. However, no studies describe surface-modified NC (pegylated approach) as reinforcement in PBAT matrices. So, this work proposes the use of PEG as a compatibilizer between NC and PBAT. The pegylated-NC improves the compatibilization of PBAT/NC nanocomposites, seeking to overcome the low interfacial adhesion between the PBAT matrix and unmodified NCs. The pegylation process was reported in our previous article. [32] Here, we show how pegylated-NCs are dispersed in the biodegradable matrix, and the possible interactions between the three components of this composite. The mechanical properties, thermal stability, crystallinity, morphological, and water absorption of the composites with and without the use of PEG were investigated.

2 | EXPERIMENTAL PROCEDURE

2.1 | Materials

Eucalyptus residues (*Eucalyptus citriodora*) were obtained after harvesting and cutting in Mato Grosso (Brazil). Sigma-Aldrich (SP, Brazil) provided the PEG (M_w = 1500 g mol^{-1}) and sodium chlorite (99%). Labsynth (SP, Brazil) provided sodium hydroxide (99%), potassium hydroxide (99%), and ethanol. BASF (SP, Brazil) provided polybutylene adipate co-terephthalate (PBAT) (M_w = 66.500 g mol^{-1}).

NC derived from eucalyptus residues was isolated and surface-pegylated according to a previously described procedure. [32] The dimensions of the NC were determined from atomic force microscopy (AFM) images, resulting in particle size between 100 and 150 nm. These particles are considered cellulose nanocrystals, and the aspect ratio (L/D) was 6.1 for the unmodified CNS, and 3.0 for pegylated-NC with 2% or 5% of PEG. Considering the NCs diameter, the values were 154, 66, and 100 nm for the samples NC, and pegylated-NC with 2% and 5%, respectively. The published article by Lima et al presents the complete characterization of pegylated-NC. [32] In this work, the surface-pegylation of the NCs was conducted in two PEG concentrations: 2 and 5 wt%. The modified samples were named NC2 and NC5, and the nonmodified NC was named NC.

2.2 | Preparation of the nanocomposites

The dried NC and the pegylated-NC were incorporated in the PBAT matrix in the proportion of 1, 3, and 5 wt% (NC: PBAT) using a Drays K-mixer MH-100 homogenizer (MH Equipamentos Ltda., Brazil). The obtained nanocomposites were compressed molded into 3.2 mm thick sheets using a hot-press at 160°C and a force of 3 tons for 3 minutes. The resulting sheets were left in the air to cool down to room temperature. The samples were named PBAT-X%NC for the unmodified samples, PBAT-X%(NC2) for the 2% surface-pegylated NCs, and PBAT-X %(NC5) for the 5% surface-pegylated NCs, where X is the amount of reinforcement used.

2.3 | Characterizations

2.3.1 | Mechanical property

The elastic modulus, elongation, and tensile strength were measured using Instron 3367 Universal Testing Machine (Norwood, EUA). The load cell and crosshead speed were 5 kN and 50 mm min^{-1}, respectively. For the tests, the sheets were cut according to ASTM D638-14, type V. The average values of Young's modulus (E), the elongation at break (ε), and the tensile strength (σ) were calculated for six specimens. The tensile test was conducted at room temperature and humidity of ~50%.

2.3.2 | Thermogravimetric analysis

Thermogravimetric analysis (TGA) was carried out using STA 6000 instrument (PerkinElmer). 10 mg of samples were heated from 20°C to 600°C at a heating rate of 20°C min^{-1} under N_2 flow (20 mL min^{-1}).

2.3.3 | Differential scanning calorimetry

An equipment differential scanning calorimeter (DSC) Q 1000 TA Instruments (New Castle, Delaware, EUA) performed DSC measurements under the nitrogen atmosphere (50 mL min^{-1}). Before the analysis, samples were weighed (5 mg) and placed into aluminum pans. The samples were heated to 200°C, cooled to −60°C and, then heated to 200°C, at a heating or cooling rate of 10°C. min^{-1}. Equation (1) calculated the nanocomposites crystallinity, where ΔH_m^0 is the melting enthalpy of 100% crystalline PBAT (114 J g^{-1}), ΔH_m is the measured enthalpy, and $W\%$ is the weight fraction of PBAT.[41]

$$Xc = 100 \times \left(\frac{\Delta H_m}{\Delta H_m^0} \times W\% \right). \quad (1)$$

2.3.4 | X-ray diffraction

The X-ray diffraction (XRD) diffractograms were obtained at ambient temperature on a STADI-P (Stoe). The operating voltage was 40 kV and a current of 40 mA, with CuKα radiation ($\lambda = 1.54056$ Å), in the range $2\theta = 5°$ to 40°. The diffraction patterns estimate the mean dimensions of the PBAT crystalline domains using the Scherrer equation (Equation (2)), where β is the peak height at half height (23.5°) (in rad), k is the diffraction wavelength ($\lambda = 1.54056$ Å), h is the diffraction angle, and K is a constant, assumed to be 0.9 due to the possible spherulitic shape of the domains. [42,43]

$$\tau = \frac{K.\lambda}{\beta.\cos\theta}. \quad (2)$$

2.3.5 | Raman spectroscopy

The nanocomposites were analyzed with a Raman spectroscopy (XRD Raman Spectroscopy Thermo Scientific, Madison). The equipment conditions were wavelength of 780 nm and a power laser of 5.0 mW, in a range of 100 to 3500 cm^{-1}, 32 scans, and spectral resolution of 4 cm^{-1}.

2.3.6 | Morphological analysis

A scanning electron microscope (FESEM) (JEOL-JSM-7200F) equipped with energy-dispersive X-ray spectroscopy (EDS) analyzed the nanocomposites fractured, with an acceleration voltage of 10 kV. The samples were sputter-coated with gold for around 5 minutes in Hummer 6.2 sputter system under 10 mA before SEM observations.

2.3.7 | Water absorption

Water absorption studies followed the ASTM D570-98 standard. Three specimens of each composition were randomly immersed in distilled water at room temperature. The samples were removed from the water after certain periods, wiped with a piece of cloth, and weighed in a high precision balance, and then submerged again in water. The weight difference calculated the water content. Equation (3) (Fick Law for water diffusion) treated the collected data, where M_t and M_∞ are the water content at "t" time and at equilibrium, respectively. The linear part of the curve obtained for log M_t/M_∞ plotted as a function of time determined the linear and angular coefficients "k" and "n," respectively.

$$\log\frac{M_t}{M_\infty} = \log(k) - n\log(t). \quad (3)$$

Equation (4) calculated the diffusion coefficient (D) of water in the nanocomposites, where L is the nanocomposite thickness.

$$\frac{M_t}{M_\infty} = \frac{4}{L}\left(\frac{D}{\pi}\right)^{0.5} t^{0.5}. \quad (4)$$

3 | RESULTS AND DISCUSSION

3.1 | Mechanical testing

Figure 1 shows the mechanical properties of the neat PBAT and its nanocomposites. Figure 1A clearly shows that the addition of the NC increased the elastic modulus (E), and the most significant NC' content was 5%, followed by 3 and 1 wt%, respectively.

For all the samples, there was a drastic decrease in the elongation at break values. The addition of NC in a polymeric matrix alters the organization of the PBAT chains and decreases their movement and elongation during tension, since the NC confine the chain motion of the polymers, reducing ε values.[24] This trend is usually reported in the literature. [33,44] The nanocomposite increase in the reinforcement phase reduces the sliding of the polymer chains. PBAT is a highly flexible polymer, so the addition of particles tends to decrease its elongation at break values. This reduction observed in all samples indicates that PEG, in the studied concentrations, did not act as a plasticizer in the polymeric matrix.

Besides, σ values decreased for all nanocomposites, and this behavior is associated with matrix-filler interface adhesion, filler content, and NC size. [45] These relationships can generate changes in several other properties, such as mechanical, thermal, and gas barrier. Tensile strength is a parameter deeply dependent on the degree dispersion of NC into the polymer matrix and can indicate that the processing was inefficient in NC dispersion. Pinheiro et al observed similar results working with modified NC as reinforcement in PBAT.[36]

Considering the modified NC samples, the addition of NC-2%P increased E values and presented intermediate σ values for all the studied composites. For NC-2%P, probably the PEG acted as a compatibilizer between the matrix and the dispersed phase, improving the nanoparticle adhesion to the matrix. Another possibility is that, due to the steric stabilization, the nanofiller is better dispersed in the PBAT matrix, decreasing the agglomeration effect, which could result in low-stress concentration. In this case, as shown in Figure 2, possibly there were interactions between the PBAT, the PEG, and the NC, improving the transfer of tension between matrix and reinforcement (Figure 1D). Figure 2 shows the studied PEG contents: 2%PEG and 5%PEG, which probably show the higher and lower adhesion between the filler and the matrix, respectively.

When incorporating NC-2%P, these nanoparticles will be partially substituted, presenting reactive points both the cellulose hydroxyls and the PEG. [46–48] These reactive points tend to interact with the PBAT carboxyl,

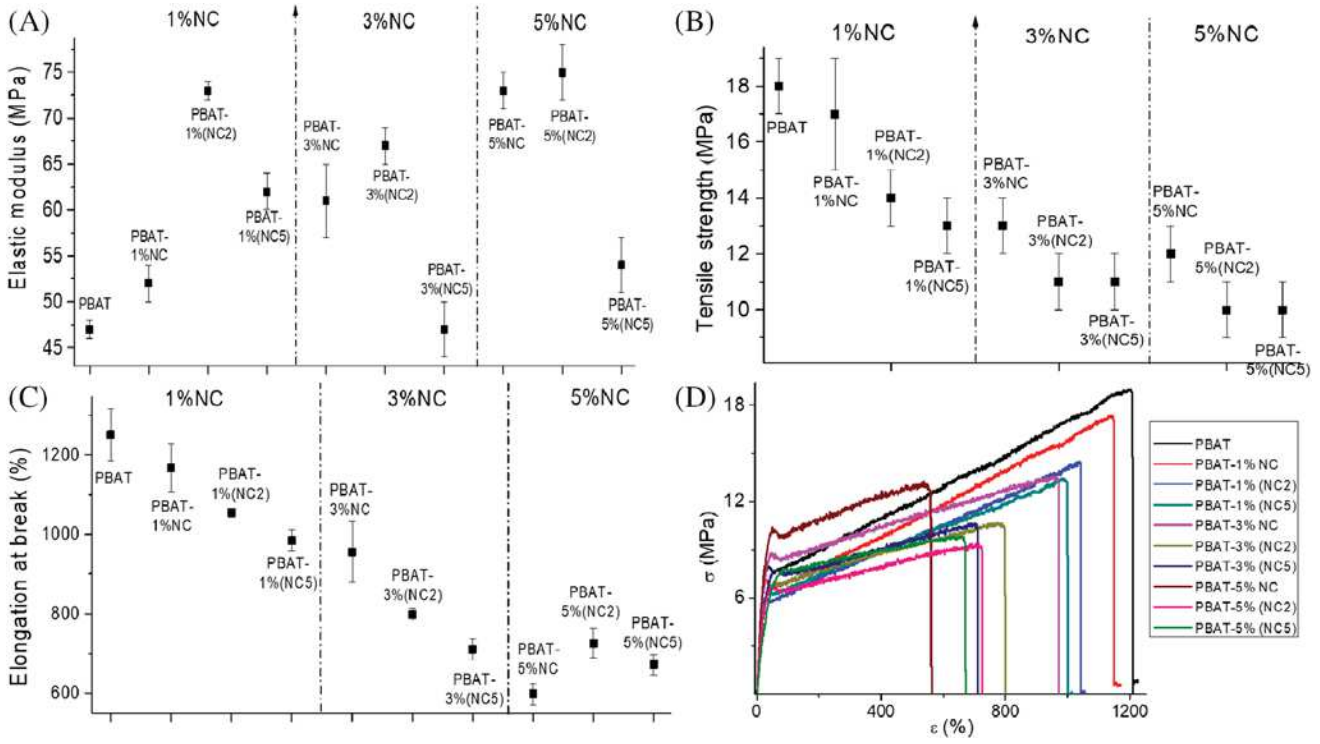

FIGURE 1 Mechanical properties of the neat PBAT and its nanocomposites: A, elastic modulus (E); B, tensile strength (σ); C, elongation at break (ε); D, representative stress–strain curves. PBAT, poly(butylene adipate-co-terephthalate) [Color figure can be viewed at wileyonlinelibrary.com]

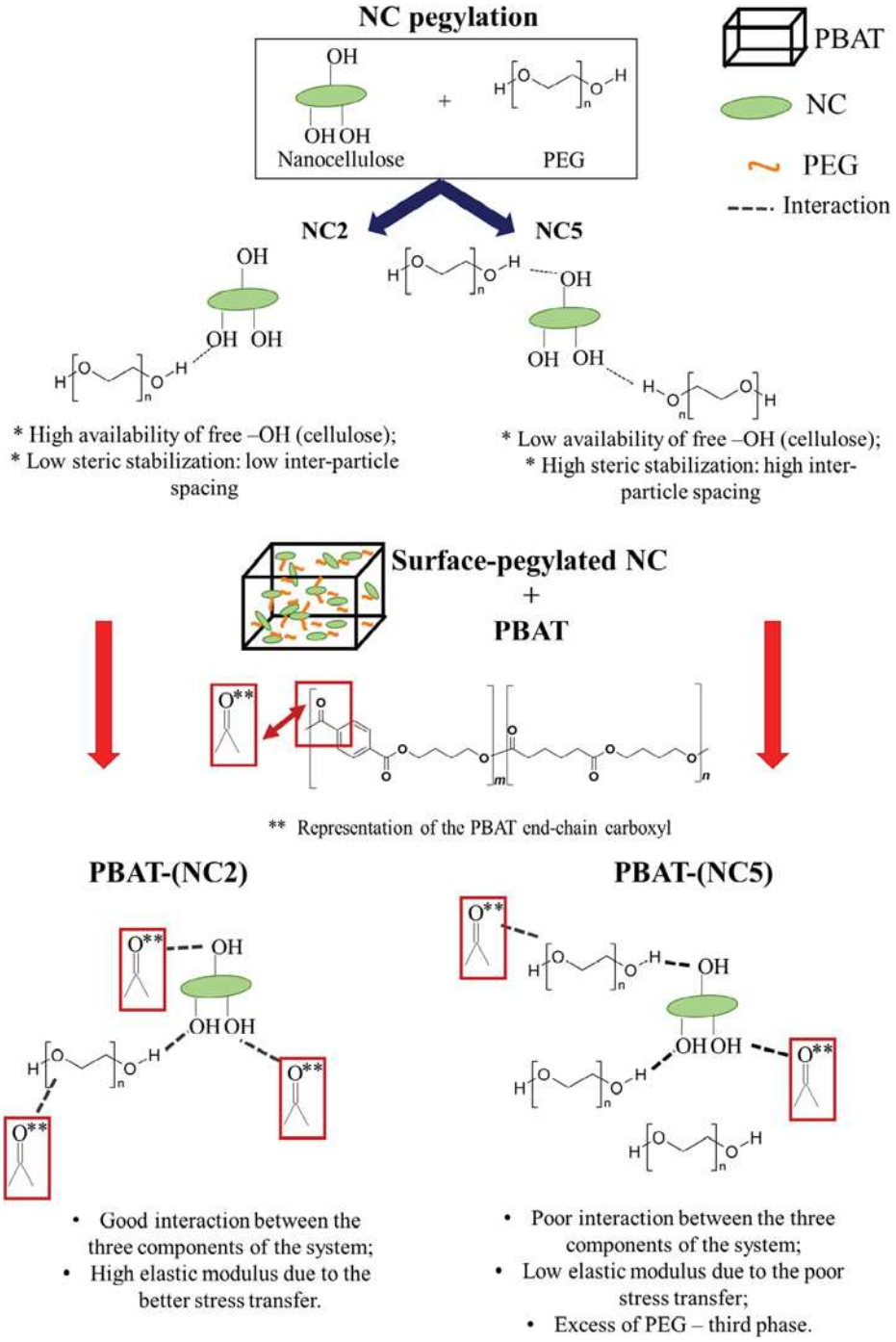

FIGURE 2 Expected interaction between the pegylated-NC and the PBAT matrix, considering the two PEG contents studied (2% and 5%). NC, nanocellulose; PBAT, poly(butylene adipate-co-terephthalate); PEG, polyethylene glycol [Color figure can be viewed at wileyonlinelibrary.com]

which can promote a better dispersion effect, caused by the pegylation, and improve the mechanical behavior of these nanocomposites. Thus, with the interactions between the three components of the system, a good transfer of tension is expected (they act as percolation paths), reflecting a significant increase in stiffness.

The mechanical results indicate that 5% of PEG hinders the interaction between matrix and reinforcement, resulting in a significant decrease in mechanical properties compared to the NC-2%P samples. In the case of 5% PEG, the NC have few reactive sites for interaction with the PBAT matrix (the cellulose hydroxyls are already interacting with the PEG), which limits their behavior as reinforcement, since only PEG interacts with the PBAT, and results in smaller increases in E values. In this case, excess PEG (chains that did not interact with NC) could result in a third phase, limiting the stress transfer between the nanocomposites components and worsening the mechanical results.

Considering the different NC contents, the PBAT-5% (NC2) sample showed the highest stiffness, followed by the PBAT-1% (NC2) sample. The addition of 3% NC

probably did not show good dispersion during processing, limiting its mechanical performance.

3.2 | Thermal properties

The thermogravimetric and the DTG curves of the neat PBAT and their nanocomposites are presented in Figure 3A,B), respectively. All samples have similar thermal behavior, with a single stage of mass loss at ~400°C, which is associated with the breakage of the C—C bonds present in the structure of the polymer. [39,49] This similarity can be attributed to two factors: (a) the concentration of nanoparticles is low compared with the total mass of the sample, which has a small influence on the polymer matrix; (b) there was a good adhesion of the reinforcement phase in the matrix. [50] It is interesting to note that the samples with 3% and 5% of NC showed a slight increase in the T_{max}, as observed in Figure 3B. According to Moustafa et al., there is possibly an interfacial interaction between the cellulose hydroxyls or the PEG with the PBAT, which increases the nanocomposites' thermal stability. [40] The interfacial bond between the reinforcement and the matrix and the compatibility between the phases

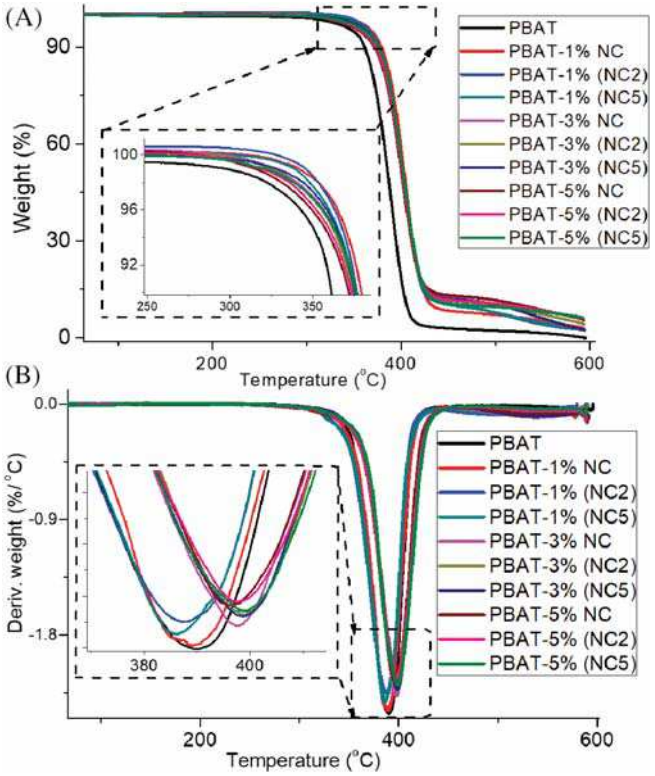

FIGURE 3 Thermal curves: A, TG and B, DTG of the neat PBAT and the studied nanocomposites. PBAT, poly(butylene adipate-co-terephthalate) [Color figure can be viewed at wileyonlinelibrary.com]

are related to the increase in the thermal stability of the nanocomposites, as was shown in Figure 2. In this case, NC can act as "cross-linking" agents, which bind the PBAT chains together, which results in higher temperatures for thermal decomposition. [37] Higher concentrations of NC require more elevated amounts of heat, which results in higher T_{max}.

Table 1 presents the DSC results for the neat PBAT and its nanocomposites, and Figure S1 presents the second heating and cooling curves, respectively. The neat PBAT and the PBAT/NC nanocomposites have a single endothermic peak, associated with the PBAT. Glass transition temperature is an important parameter in the composites technology that explains the miscibility or immiscibility of polymer composites.[51] While non-modified NC did not show a significant change in T_g values, pegylated-NC decreased the T_g values by ~4°C, which indicates good miscibility between the PBAT matrix and the reinforcement.[40,52] Different from the mechanical results, this decrease indicates a possible plasticizer effect.[53]

The melting temperature of neat PBAT was 124°C and increased ~3°C after the NC addition, and after the addition of the pegylated-NC, it was observed a new peak at approximately 40°C. This peak may be related to the melting temperature of PEG.

This increase means more thermal energy is needed to undo the material's crystalline structure and make it viscous. An increase in T_m implies that the polymer can be processed at slightly higher temperatures without the risk of degradation. This increase can be associated with different forms of crystallites, caused by the insertion of nanoparticles, different crystalline organizations, possible molecular orientation, and possible segregation effects, caused by differences in composition.

The difference in T_c values is significant with an increase (from 80 to ~100°C) after the addition of the nanoparticles. The addition of NC and pegylated-NC acts as heterogeneous nucleation by increasing nucleation sites that promote the crystallization of PBAT [54]. In this case, the polymeric crystals cover the surface of the NC. For these samples, the crystallite size is smaller than that of neat PBAT due to the physical limitation of crystallites growth created by the numerous nucleation point, which justifies the slight decrease in the crystallinity values (Figure 4)., except for PBAT-1%NC and PBAT/5%(NC5).

The X_c decrease occurred due to the NC, which restricted the polymer chain movement, decreasing the crystallization of the PBAT chains. [37] Briefly, it is possible to conclude that the NC dominates the nucleation process the overall, in other words, the crystallization of the system. Besides, there is no strong "confinement" of

Samples	T_g (°C)	$T_{m\ PEG}$ (°C)	$T_{m\ PBAT}$ (°C)	T_c (°C)	X_c (%)	τ (nm)
PBAT	−32.2	—	124.2	79.9	9.4	11.4
PBAT-1%NC	−35.0	—	127.1	91.1	11.3	11.3
PBAT/1%(NC2)	−30.5	37.8	127.0	91.3	7.1	.9.3
PBAT/1%(NC5)	−29.8	37.6	127.1	91.2	7.3	9.8
PBAT/3%NC	−34.1	—	126.8	98.2	8.4	7.6
PBAT/3%(NC2)	−35.6	38.0	128.5	107.0	6.8	7.7
PBAT/3%(NC5)	−35.5	37.8	127.1	104.7	8.9	8.5
PBAT/5%NC	−34.5	—	127.3	101.9	7.5	7.7
PBAT/5%(NC2)	−36.3	38.5	128.8	106.6	5.8	7.6
PBAT/5%(NC5)	−36.0	38.4	127.1	104.2	10.8	7.7

Abbreviations: NC, nanocellulose; PBAT, poly(butylene adipate-co-terephthalate); PEG, polyethylene glycol.

TABLE 1 DSC results for PBAT, and PBAT nanocomposites with 1, 3 and 5 wt% of unmodified NC and surface-pegylated-NC, and crystallite size (τ) of neat PBAT and their nanocomposites, calculated by Scherrer equation

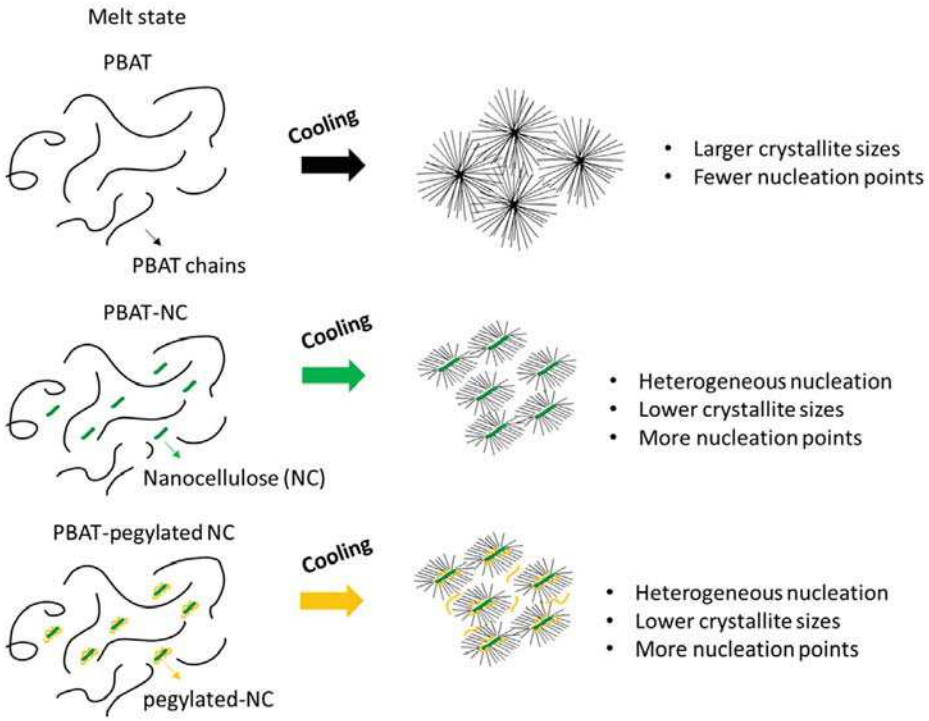

FIGURE 4 Illustration of possible interaction of PBAT, PBAT-NC, and PBAT-pegylated-NC and the expected behavior of the polymer crystallization with and without the nanocellulose. NC, nanocellulose; PBAT, poly(butylene adipate-co-terephthalate) [Color figure can be viewed at wileyonlinelibrary.com]

the nanoparticles in polymer chains. That is, there was no considerable variation in how nucleation occurs and in the growth of the crystallites, and therefore there was no significant variation in the nanocomposite crystallinity. [38]

3.3 | X-Ray diffraction

Figure 5 shows the diffraction patterns of PBAT samples and their nanocomposites. Neat PBAT exhibits five different peaks of crystallinity, being a combination of amorphous and crystalline structures. The crystalline peaks are observed at 16.3°, 17.7°, 20.5°, 23.3°, and 24.9°. There is no significant transcrystalline phase at the interface of the system, that is, there are no significant structural changes in PBAT that have been induced by NC. [34] No new diffraction peaks were found in the XRD patterns, possibly because PBAT is in a much higher concentration than NC. However, samples with 5% NC showed a weak signal at ∼34.5°, which can be attributed to the cellulose phase.[18,55]

The diffraction patterns were used to estimate the mean dimensions of the PBAT crystalline domains using the Scherrer equation, as described in the experimental section. Table 1 shows the results of the crystallite size.

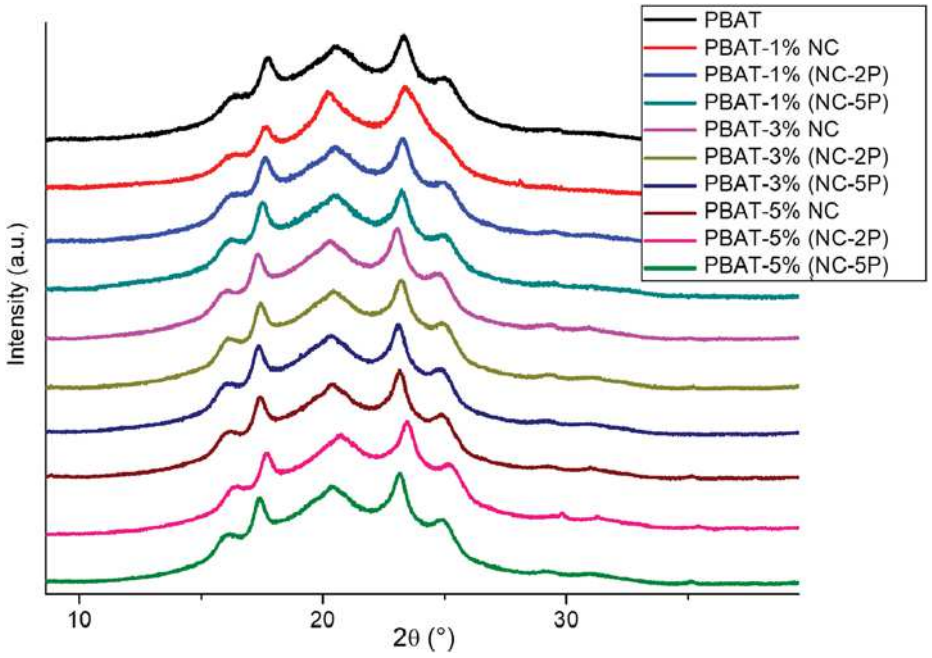

FIGURE 5 XRD patterns of neat PBAT and their nanocomposites. PBAT, poly(butylene adipate-co-terephthalate); XRD, X-ray diffraction [Color figure can be viewed at wileyonlinelibrary.com]

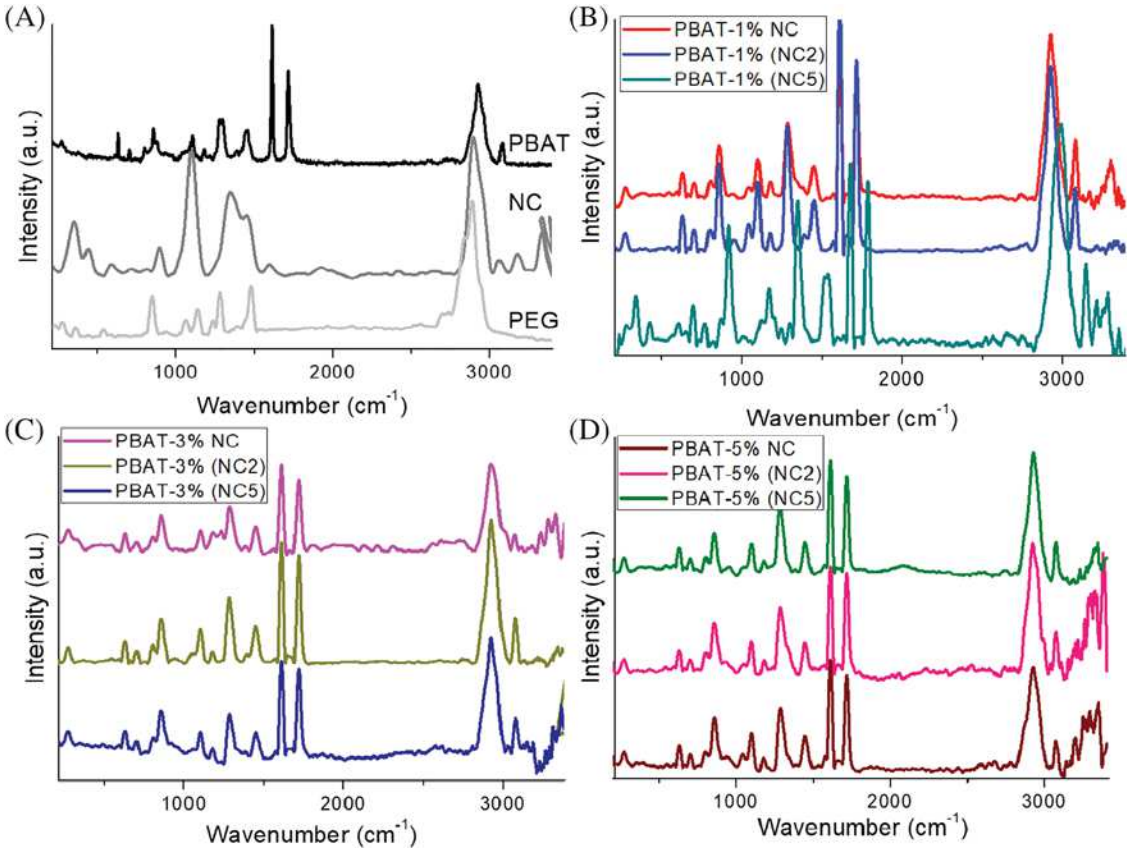

FIGURE 6 Raman spectra of A, raw materials—PBAT, NC, and PEG, and PBAT nanocomposites with nonpegylated and pegylated-NC in the different contents of B, 1%; C, 3%; and D, 5%. NC, nanocellulose; PBAT, poly(butylene adipate-co-terephthalate); PEG, polyethylene glycol [Color figure can be viewed at wileyonlinelibrary.com]

The decrease in τ indicates that the presence of nanoparticles has a strong influence on the crystallization of PBAT matrix, promoting nucleation and preventing the growth of crystallites, as shown in Figure 4. [56] Such results are consistent with those observed by the DSC, where there is a decrease in crystallinity as the pegylated-NC content increases. [42]

3.4 | Raman spectroscopy

Raman spectroscopy accessed the nature of functional groups and their interaction with the neighboring groups. [57] Figure 6A-D shows the Raman spectra of the raw materials (PBAT, NC, and PEG) and the developed nanocomposites. In Figure 6A, it is possible to verify the main peaks of each sample. The main vibrational frequencies of the PBAT appeared at 640 to 860 cm^{-1} (aromatic ring vibrations), 1100 to 1285 cm^{-1} (aromatic —C—H stretching), 1461 cm^{-1} (—C═O stretching), 1618 cm^{-1} (—CH_2 stretching), 1720 cm^{-1} (—C═C stretching), and 3085 cm^{-1} (C—O—C stretching). [57] The Raman spectra of cellulose showed the main peaks at 380 and 460 cm^{-1} (C—C—C, C—O, and C—C—O ring deformation), 900 cm^{-1} (C—H ring of cellulose), 1456 cm^{-1} (H—C and H—O—C bending), 1300 to 1500 cm^{-1} (—CH_2 and —CH_2OH deformations), 2889 cm^{-1} (CH and CH_2 stretching), and 3286 to 3402 cm^{-1} (O—H stretch). [58,59]

Due to the similarity between the PBAT and NC spectra and the low content of NC used, it is not possible to identify characteristic cellulosic peaks in the nanocomposite spectra. Some peaks showed larger and less defined after the addition of NC, which can be associated with the influence of the NC structure. [60] The addition of NC-5% PEG resulted in a shift in the vibrational frequencies (~10-20 cm^{-1}), which suggests that there is an interaction between the components of the mixture.

According to Agarwal et al, shifts of the 1095 cm^{-1} band result from the uniaxial deformation of nanocomposites. [61] In this work, all the nanocomposites showed shifts between 1 and 3 cm^{-1}, which are indicative of the stress transfer between the PBAT and the NC due to strong interfacial hydrogen bonding, which are responsible for increases in the elastic modulus, [58] as presented in the mechanical results. In general, the PBAT-NC showed shifts of 2 cm^{-1}. The PBAT-(NC-2%P) showed variations of 3 cm^{-1}, and PBAT-(NC-5%P) presented shifts of 10 cm^{-1}. Small changes in the vibrational frequency of the composites can be associated with chemical interactions between the active groups of the components (ie, hydroxyls from cellulose and PEG, and carboxyl groups of PBAT), as demonstrated in the mechanical results. These interactions are possible of the hydrogen bonding type, since there are no new peaks, and the approximation of the chains alters the conformation of the polymer chains and, consequently, their modes of vibration and deformation. Therefore, higher amounts of NC (5%) have more points of interaction, thus causing higher peak shifts. This interaction is responsible for the increase in the stiffness of the composite.

3.5 | Morphological analysis

The fracture surface of samples, including PBAT nanocomposites with pegylated and nonpegylated-NC as a function of different contents, were observed by FESEM. Figure 7 shows the morphology of the studied samples, and the white dots were identified in the PBAT matrix, which corresponds to the NC-matrix in the perpendicular plane of the nanocomposite. [17]

The PBAT-NC samples showed a good dispersion of the nanoparticles. A lot of empty spaces (cavities) can be observed (indicated by the red circles), which means that the adhesion of the NC in the matrix was poor. [1]

The samples 2% pegylated-NC showed good compatibility between the nanoparticles and the polymeric matrix, which was evaluated by the "broken" NC particles (indicated by the yellow circles and arrows). It represents an efficient stress transfer by the higher NC's capacity to absorb energy. [17] Some NC particles appear to be embedded in the PBAT matrix rather than exposed at the surface, suggesting good compatibility and adhesion. [6] Furthermore, no debonding of the nanoparticles from the matrix was observed, implying functional interactions,[1] as discussed in Figure 2. Probably a percolating network structure was formed due to the interactions among PBAT-NC-PEG, as reported previously.

The samples 5% pegylated-NC showed an intermediary behavior, with cavities and nanoparticles. In this case, the holes are possibly due to the formation of a separate phase of PEG.[6] This phase is associated with the PEG excess, as mentioned before.

3.6 | Water absorption

All nanocomposites have a similar water absorption behavior, with higher absorption in the first few hours, and then there is a stabilization (equilibrium). Figure 8 shows that the nanocomposites differ in the intensities of water absorption. Equation (3) was applied to understand the water absorption behavior of the samples, and Table 2 presents the calculated parameters. When n is close to 0.5, the samples have favorable conditions for the

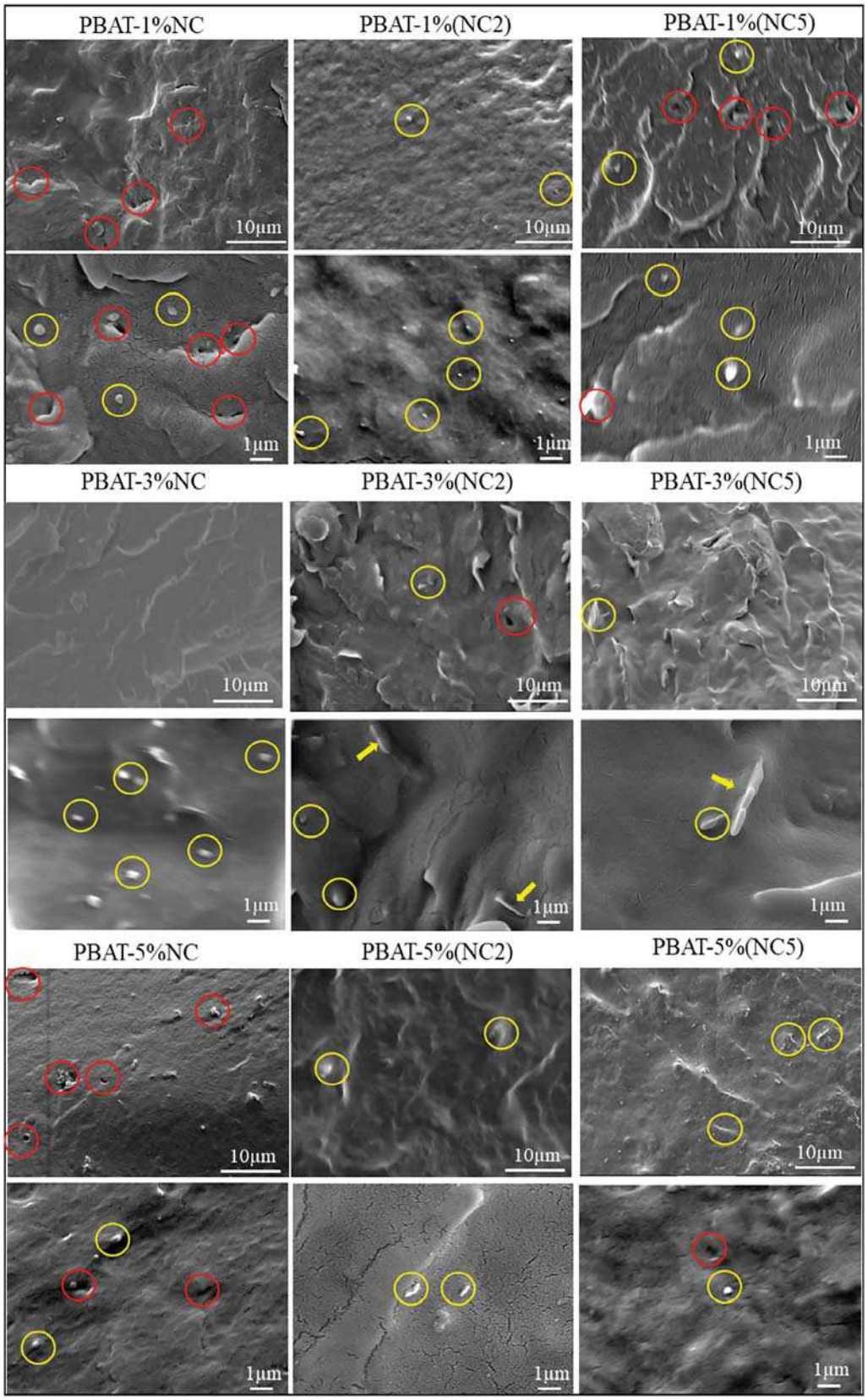

FIGURE 7 SEM micrographs of PBAT nanocomposites. The red circles indicate surface cavities due to the poor adhesion between the phases, and the yellow circles are associated with the presence of NCs in the matrix, resulting in good adhesion between the matrix and the NC. NC, nanocellulose; PBAT, poly(butylene adipate-co-terephthalate) [Color figure can be viewed at wileyonlinelibrary.com]

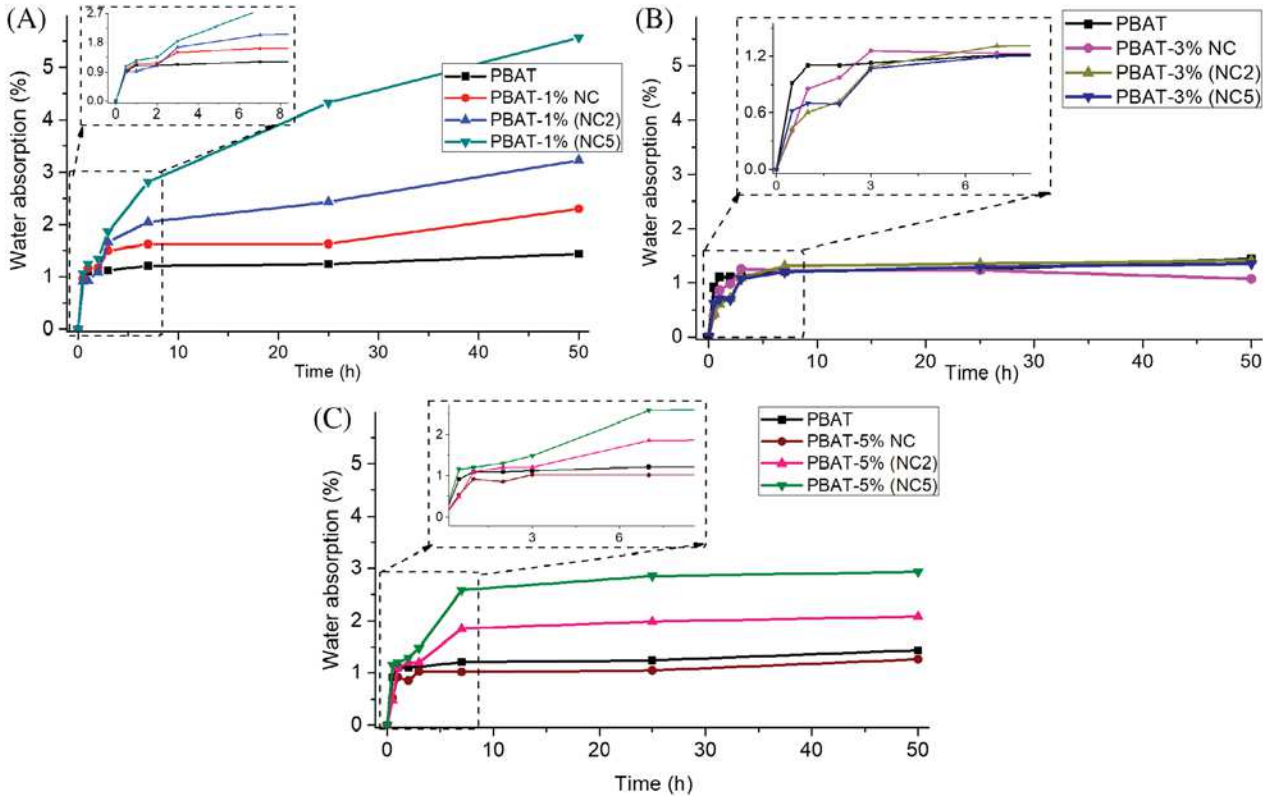

FIGURE 8 Water absorption isotherm curves (% wt gain) for PBAT and their nanocomposites: A, 1%; B, 3%; and C, 5% nonpegylated and pegylated-NC. NC, nanocelluose; PBAT, poly(butylene adipate-co-terephthalate) [Color figure can be viewed at wileyonlinelibrary.com]

TABLE 2 Diffusion parameters *k*, *n*, and diffusion coefficient (*D*) for the PBAT and their nanocomposites

Samples	*k*	*n*	D (m^2/s) × 10^{13}
PBAT	−1.90	0.50	2.56
PBAT-1%NC	−2.47	1.16	2.32
PBAT/1%(NC2)	−2.15	0.53	2.21
PBAT/1%(NC5)	−2.28	0.45	1.63
PBAT/3%NC	−0.58	0.62	9.84
PBAT/3%(NC2)	−0.74	0.22	8.23
PBAT/3%(NC5)	−0.94	0.47	8.11
PBAT/5%NC	−0.43	0.32	10.6
PBAT/5%(NC2)	−0.61	0.02	8.71
PBAT/5%(NC5)	−0.63	0.10	8.83

Abbreviations: NC, nanocellulose; PBAT, poly(butylene adipate-co-terephthalate).

application of Fick's Law. All the samples showed favorable conditions, so the Fick's Law was applied.

The value of *k* represents the material affinity with water molecules, and the higher the value of *k*, the greater the interaction of the polymer with water. This affinity is associated with polymer hydrophilicity, and low values are attributed to higher hydrophobicity. In this case, considering 1% NC, as the NC interacted with PBAT active groups, the hydrophilic groups are not available to bond with water, decreasing the water absorption. However, this trend reversed to the higher contents of NC. Considering 3% and 5% NC, there is a high content of cellulose free hydroxyls, which are hydrophilic, justifying the increase of hydrophilicity of the nanocomposite. In the case of pegylated-NC, it was observed that NC2 has a higher uptake tendency, followed by the NC5P samples.

The diffusion coefficient showed a similar trend; this is the most important parameter of the Fick model, demonstrating the ability of solvent molecules (water, in the study, considered), to penetrate the nanocomposite's structure. The nonpegylated-NC showed the highest values of D; this parameter is influenced by the free hydroxyls and the voids in the interfacial region between the reinforcement and the matrix. [62] As observed in the scanning electron microscopy (SEM) images (Figure 7), there is a low adhesion between the NC and the PBAT, which may result in cavities that influence the absorption of water.

Another hypothesis is that PEG slows the diffusion of water in the bulk of the material. The interaction of the cellulose hydroxyls with the PEG hydroxyls results in fewer hydrophilic groups available, thereby reducing the

affinity of the material with water and the diffusion coefficient. This tendency is observed mainly for samples with 3% and 5% NC, at both studied concentrations of PEG.

The addition of PEG was more impacting for the sample of 1% NC, resulting in behavior different from the other compositions studied, as shown in the mechanical properties, where there was a more significant increase in stiffness compared with the sample nonpegylated. Pegylation was effective in increasing compatibility between the reinforcement and the matrix, especially at low filler concentrations.

These water absorption results are essential because they can give an initial idea of the behavior of the materials during the hydrolysis, which is an abiotic degradation in which the material is degraded only by water.

4 | CONCLUSIONS

The addition of nonpegylated-NC resulted in a discrete increase in the material's stiffness, without significant improvements in other properties, which is an indication that they did not act as reinforcement and that there were poor compatibility and adhesion between the matrix and NC. The pegylated-NC in the PBAT matrix resulted in a significant increase in the material's stiffness, especially the 2% pegylated-NC nanocomposites. A similar trend was observed for all the contents of NC studied (1, 3, and 5 wt%). The addition of modified NC improved the dispersion and adhesion of the nanoparticles in the matrix. Stiffness is associated with hydrogen bonds between the NC and PEG hydroxyls and the PBAT carboxylates. The 5% pegylated-NC showed limited mechanical performance, which is related to the excess of PEG, which formed a separate phase in the nanocomposites. There was an increase in thermal stability, which is a result of interfacial interactions between materials.

The nanocomposites decreased the degree of crystallinity, probably due to the nucleation effect that the nanoparticles exert during the cooling of the polymer, reducing the crystallite sizes. By evaluating the mechanical properties and the thermal properties, it was observed that the addition of 2% pegylated-NC decreases the nanocomposite crystallinity but presents the best mechanical properties. In this sample, the increase of stiffness is related to the interface formed between the matrix and reinforcement, which generated good adhesion and tension transfer. The nanocomposites present the enormous potential of application in different products, ranging from areas, such as food packaging to biomedicine and agricultural materials.

ACKNOWLEDGMENT

The authors thank the financial support provided by FAPESP (2018/11277-7, 22035-4 and 2018/25239-0), CNPq, CAPES, NSF-CREST #1735971, and the Multiuser Experimental Center of the Federal University of ABC (CEM-UFABC).

ORCID

Derval dos Santos Rosa https://orcid.org/0000-0001-9470-0638

REFERENCES

[1] J. K. Muiruri, S. Liu, W. S. Teo, J. Kong, C. He, *ACS Sustain. Chem. Eng.* **2017**, *5*, 3929.
[2] B. Bittmann, R. Bouza, L. Barral, M. V. Gonzalez-Rodriguez, M.-J. Abad, *Polym. Compos.* **2008**, *16*, 101.
[3] N. M. Barkoula, B. Alcock, N. O. Cabrera, T. Peijs, *Polym. Compos.* **2009**, *31*, 1194.
[4] M. Gu, C. Jiang, D. Liu, N. Prempeh, I. I. Smalyukh, *ACS Appl. Mater. Interfaces* **2016**, *8*, 32565.
[5] P. Bertsch, S. Isabettini, P. Fischer, *Biomacromolecules* **2017**, *18*, 4060.
[6] A. Boujemaoui, C. Cobo Sanchez, J. Engström, C. Bruce, L. Fogelström, A. Carlmark, E. Malmström, *ACS Appl. Mater. Interfaces* **2017**, *9*, 35305.
[7] K. H. Lee, G. Yang, B. E. Wyslouzil, J. O. Winter, *ACS Appl. Polym. Mater.* **2019**, *1*, 691
[8] W. J. Lee, A. J. Clancy, E. Kontturi, A. Bismarck, M. S. P. Shaffer, *ACS Appl. Mater. Interfaces* **2016**, *8*, 31500.
[9] N. A. M. Razali; E. M. Salleh; R. N. I. R Othman; L. Jasmani; S. Zakaria; F. A Aziz, in *AIP Conf. Proc.*,Feb **2019**, 2068. https://doi.org/10.1063/1.5089364.
[10] A. Dufresne, *Curr. For. Reports* **2019**, *5*, 76.
[11] J. Torstensen, R. M. L. Helberg, L. Deng, Ø. W. Gregersen, K. Syverud, *Int. J. Greenh. Gas Control* **2019**, *81*, 93.
[12] F. Valentini, A. Dorigato, D. Rigotti, A. Pegoretti, *J. Polym. Environ.* **2019**, *27*, 1333.
[13] L. K. Kian, N. Saba, M. Jawaid, M. T. H. Sultan, *Int. J. Biol. Macromol.* **2019**, *121*, 1314.
[14] E. Vatansever, D. Arslan, M. Nofar, *Int. J. Biol. Macromol.* **2019**, *137*, 912.
[15] J. C. Natterodt, J. Sapkota, E. J. Foster, C. Weder, *Biomacromolecules* **2017**, *18*, 517.
[16] E. Abraham, B. Deepa, L. A. Pothan, M. Jacob, S. Thomas, U. Cvelbar, R. Anandjiwala, *Carbohydr. Polym.* **2011**, *86*, 1468.
[17] Y. Li, H. Chen, D. Liu, W. Wang, Y. Liu, S. Zhou, *ACS Appl. Mater. Interfaces* **2015**, *7*, 12988.
[18] F. Ferreira, I. F. V; Pinheiro, R. F. Gouveia, G. P. Thim, L. M. F. Lona, *Polym. Compos.* **2018**, *39*, E9
[19] W. Dong, H. Hakukawa, N. Yamahira, Y. Li, S. Horiuchi, *ACS Appl. Polym. Mater.* **2019**, *1*(4), 815.
[20] H. Chen, X. Yan, Q. Feng, P. Zhao, X. Xu, D. H. L. Ng, L. Bian, *ACS Sustain. Chem. Eng.* **2017**, *5*, 11387.
[21] E. M. Fernandes, R. A. Pires, J. F. Mano, R. L. Reis, *Prog. Polym. Sci.* **2013**, *38*, 1415.
[22] S. X. Peng, S. Shrestha, Y. Yoo, J. P. Youngblood, *Polymer* **2017**, *112*, 359.

[23] S. Nagarajan, J. Hu, H. Wu, Y. Duan, J. Zhang, *Polymer* **2018**, *150*, 184.
[24] C. Peng, Q. Yang, W. Zhao, J. Ren, Q. Yu, Y. Hu, X. Zhang, *Compos. Sci. Technol.* **2019**, *177*, 103.
[25] E. Kloser, D. G. Gray, *Langmuir* **2010**, *26*, 13450.
[26] J. Araki, M. Wada, S. Kuga, *Langmuir* **2001**, *17*, 21.
[27] A. K. Sudari, A. A. Shamsuri, E. S. Zainudin, P. M. Tahir, *J. Thermoplast. Compos. Mater.* **2017**, *30*, 855.
[28] A. G. Cunha, J. B. Mougel, B. Cathala, L. A. Berglund, I. Capron, *Langmuir* **2014**, *30*, 9327.
[29] B. L. Tardy, S. Yokota, M. Ago, W. Xiang, T. Kondo, R. Bordes, O. J. Rojas, *Curr. Opin. Colloid Interface Sci.* **2017**, *29*, 57.
[30] R. F. S. Barbosa, A. G. Souza, D. S. Rosa, *Polym. Compos.* **2020**, *71*, 2841
[31] T. Kaldéus, M. Nordenström, A. Carlmark, L. Wågberg, E. Malmström, *Carbohydr. Polym.* **2018**, *181*, 871.
[32] G. F. Lima, A. G. Souza, D. S. Rosa, *J. Mol. Liq.* **2018**, *268*, 415.
[33] C. L. Morelli, M. N. Belgacem, M. C. Branciforti, M. C. B. Salon, J. Bras, R. E. S. Bretas, *Polym. Eng. Sci.* **2016**, *56*, 1339.
[34] T. Mukherjee, M. Czaka, N. Kao, R. K. Gupta, H. J. Choi, S. Bhattacharya, *Carbohydr. Polym.* **2014**, *102*, 537.
[35] X. Zhang, P. Ma, Y. Zhang, *Polym. Bull.* **2016**, *73*, 2073.
[36] I. F. Pinheiro, F. V. Ferreira, D. H. S. Souza, R. F. Gouveia, L. M. F. Lona, A. R. Morales, L. H. I. Mei, *Eur. Polym. J.* **2017**, *97*, 356.
[37] S. K. Rahimi, R. Aeinehvand, K. Kim, J. U. Otaigbe, *Biomacromolecules* **2017**, *18*, 2179.
[38] M. Mariano, N. Kissi, A. Dufresne, *Langmuir* **2016**, *32*, 10093.
[39] H. Moustafa, C. Guizani, C. Dupont, V. Martin, M. Jeguirim, A. Dufresne, *ACS Sustain. Chem. Eng.* **2017**, *5*, 1906.
[40] H. Moustafa, C. Guizani, A. Dufresne, *J. Appl. Polym. Sci.* **2017**, *134*, 1.
[41] E. d. C. Nunes, A. G. de Souza, D. d. S. Rosa, *J. Compos. Mater.* **2020**, *54*.
[42] M. Mariano, C. Chirat, N. El Kissi, A. Dufresne, *J. Polym. Sci. Part B Polym. Phys.* **2016**, *54*, 2284.
[43] L. N. Ludueña, E. Fortunati, J. I. Morán, V. A. Alvarez, V. P. Cyras, D. Puglia, L. B. Manfredi, M. Pracella, *J. Appl. Polym. Sci.* **2016**, *133*, 1.
[44] K. Fukushima, A. Rasyida, M. C. Yang, *Appl. Clay Sci.* **2013**, *180*, 291.
[45] J. Yang, C.-R. Han, J.-F. Duan, F. Xu, R.-C. Sun, *ACS Appl. Mater. Interfaces* **2013**, *5*(5), 3199.
[46] G. Jiang, M. Zhang, J. Feng, S. Zhang, X. Wang, *ACS Sustain. Chem. Eng.* **2017**, *5*, 11246.
[47] F. Sun, H. R. Nordli, B. Pukstad, E. Kristofer Gamstedt, G. Chinga-Carrasco, *J. Mech. Behav. Biomed. Mater.* **2017**, *69*, 377.
[48] H. Sun, X. Shao, Z. Ma, *J. Food Sci.* **2016**, *81*, E2529.
[49] S. Mohanty, S. K. Nayak, *J. Polym. Environ.* **2012**, *20*, 195.
[50] X. Wang, P. Qu, L. Zhang, *Fibers Polym.* **2014**, *15*, 302.
[51] T. Jayaramudu, H. U. Ko, H. C. Kim, J. W. Kim, E. S. Choi, J. Kim, *Compos. Part B Eng.* **2019**, *156*, 43.
[52] L. Martino, M. A. Berthet, H. Angellier-Coussy, N. Gontard, *J. Appl. Polym. Sci.* **2015**, *132*, 1.
[53] A. K. Pal, F. Wu, M. Misra, A. K. Mohanty, *Compos. Part B Eng.* **2020**, *198*, 108141.
[54] L. Liu, Y. Zhang, F. Lv, B. Yang, X. Meng, *Polym. Polym. Compos.* **2008**, *16*, 101.
[55] H. Moustafa, A. M. Youssef, N. A. Darwish, A. I. Abou-Kandil, *Compos. Part B Eng.* **2019**, *172*, 16.
[56] S. Feng, D. Wu, H. Liu, C. Chen, J. Liu, Z. Yao, J. Xu, M. Zhang, *Thermochim. Acta* **2014**, *587*, 72.
[57] M. C. Biswas, S. Jeelani, V. Rangari, *Compos. Commun.* **2017**, *4*, 43.
[58] U. P. Agarwal, *Handbook of Nanocellulose and Cellulose Nanocomposites*, Wiley-VCH Verlag GmbH & Company, Nova Jersey, EUA **2017**, p. 609.
[59] J. S. Lupoi, E. Gjersing, M. F. Davis, *Front. Bioeng. Biotechnol.* **2015**, *3*, 50.
[60] D. Roy, A. P. Kotula, B. Natarajan, J. W. Gilman, D. M. Fox, K. B. Migler, *Polymer* **2018**, *153*, 70.
[61] U. P. Agarwal, *Nanocelluloses: Their Preparation, Properties, and Applications*, 1251, ACS Publications, Washington, DC **2017**, p. 75.
[62] A. Espert, F. Vilaplana, S. Karlsson, *Compos. Part A Appl. Sci. Manuf.* **2004**, *35*, 1267.

SUPPORTING INFORMATION

Additional supporting information may be found online in the Supporting Information section at the end of this article.

How to cite this article: de Souza AG, de Lima GF, Rangari VK, dos Santos Rosa D. Investigation of surface-pegylated nanocellulose as reinforcing agent on PBAT biodegradable nanocomposites. *Polymer Composites*. 2020;41: 4340–4352. https://doi.org/10.1002/pc.25716